"Study of Combustion Mechanism of Nitramine-Polymer Mixtures"

Final Technical Report
by
Anatoli A.Zenin

November, 1998

United States Army

EUROPEAN RESEARCH OFFICE OF THE U.S.ARMY

London, England

CONTRACT NUMBER N68171-97-M-5771

Russian Academy of Sciences,
Semenov Institute of Chemical Physics

Approved for Public Release; distribution unlimitec

REPORT DOCUMENTATION PAGE

1. AGENCY USE ONLY	2. REPORT DATE	3. REPORT TYPE AND DATES COVERED
	15 November 1998	Final Report; 15 September '97 - 15 November '98

4. TITLE AND SUBTITLE

"Study of Combustion Mechanism of Nitramine-Polymer Mixtures"

5. FUNDING NUMBERS

C

6. AUTHOR

Anatoli A. Zenin

7. PERFORMING ORGANISATION NAME AND ADDRESS

Senenov Institute of Chemical Physics, Russian Academy of Sciences
Kosygin Street 4, 117977 Moscow, Russia

8. PERFORMING ORGANISATION REPORT NUMBER

-

9. SPONSORING/MONITORING AGENCY NAME AND ADDRESS

Naval Regional Contracting Center. Detachment London, Block 2, Wing 11.
DoE Complex, Eastcote Road, Ruislip, MIDDX, UK, HA4 8BS
Todd McKamey

10. SPONSORING/MONITORING AGENCY REPORT NUMBER

11. SUPPLEMENTARY NOTES

12a. DISTRIBUTION/AVAILABILITY STATEMENT

12b. DISTRIBUTION CODE

13. ABSTRACT

Combustion mechanism of mixtures of RDX- and HMX-copolymer (like HTPB) was investigated by microthermocouple techniques. The following parameters were found and analysed at different pressures, sample initial temperatures and oxidizer content: burning rates, burning surface temperatures, temperatures and sizes of different zones of combustion waves, thickness of heat and melted layers in solid, characteristic thickness and conductive sizes in the gas phase, heat release in solid, heat feedback from gas to solid, heat release rate in gas, macrokinetic laws of solid gasification, temperature sensitivities of burning rate and burning surface temperature. It was established that the significant heat release in solid and the weak heat feedback from gas to solid are observed for all mixtures. The control region in the combustion waves which governs the burning rate is placed in solid and in a thin gas layer close to surface. It was found that increase of the amount of oxidizer in the mixtures decreases temperature sensitivities of burning rate and burning surface temperature for both oxidizers.

14. SUBJECT ITEMS

RDX- and HMX-copolymer mixtures, combustion mechanism, temperature profiles of combustion waves, burning wave parameters, heat release in solid, head feedback from gas to solid, macrokinetics of gasification, burning rate control region, temperature sensitivities of burning rate and burning surface temperature.

15. NUMBER OF PAGES

16

16. PRICE CODE

NTIS

17. SECURITY CLASSIFICATION OF REPORT	18. SECURITY CLASSIFICATION OF THIS PAGE	19 SECURITY CLASSIFICATION OF ABSTRACT	20. LIMITATION OF ABSTRACT
UNCLASSIFIED	UNCLASSIFIED	UNCLASSIFIED	UL

Body of the Report

Statement of the Problem and Background

Cyclic nitramines (RDX and HMX) offer many advantages for advanced propulsions. They have better performances (large amount of gas, high specific impulse for rockets and impetus for guns), safety (low sensitivity) and environment friendness (nontoxic and noncorrosive combustion products). Modern propellants containing the nitramines and binders are named LOVA (low vulnerability in air). The study of the new propellants (or - nitramine-polymer mixtures) is very important: understanding of the combustion mechanism of these mixtures can be helpful in solving a number of practical problems.

Approach

In the first part of the study (which comprises the work of the contract) a representative simple binder was used for preparing polymer-nitramine mixtures: copolymer of butadiene and isoprene with hydroxyl terminated groups (CBIH). CBIH is similar to HTPB: the structure CBIH is distinguished from HTPB only by isoprene groups (their inclusion increases elastic characteristics of the polybutadiene binder). In this work we will use for the binder nomination HTPB1, instead of CBIH. Mixtures were prepared on the base of HMX and RDX. The main part of the investigations was performed for mixtures having small or bimodal nitramine particle sizes and various nitramine content. The study of the combustion mechanism of the mixtures was performed by obtaining geometrical and thermal structure of burning waves of the mixtures and by processing of the obtained data. The peculiarity of the work is the measurement of all the characteristics of combustion waves under changes of external parameters - initial sample temperature and pressure. This approach allows one to established distinctive features of the combustion mechanism of the studied mixtures, including differential characteristics of the burning wave parameters and macrokinetics of the control stage.

Experimental Techniques.

Temperature profiles of the combustion waves and the burning surface temperatures were obtained by microthermocouple methods. Profiles of the combustion waves were obtained by microthermocouples imbedded into solid. Thermocouples went through combustion waves when the waves propagated through the solid samples and registered temperature profiles. The ribbon U-shaped thermocouples made of alloys W+5%Re/W+20%Re of 2-7mkm thick were imbedded into the samples. Every sample had inside 2-3 thermocouples placed one above the other. Distances between the junctions were 2-4 mm. The samples were burned in a bomb of constant pressure in atmosphere of nitrogen at pressures 1(5)-80atm and at sample initial temperatures T_0=+20, and +100°C. In experiments at elevated sample temperatures the sample was placed into a small thermostat inside the bomb. The sample heating was controlled by thermocouples. Samples were ignited by electrically heated wire. Thermocouple signals were registered by amplifier and oscillograph. Burning rate was measured by time delay between the thermocouple signals, by photoregistrations of sample combustion and by pressure increase during the sample combustion. Photoregistration of sample combustion allows also the type of combustion to be established. Burning surface temperatures were measured by thermocouples that are being pressed to the surface during sample combustion and by establishing the locations of slope breaks on temperature profiles registered by thermocouples (see below).

Temperature Profile Measurement Validation.

As a rule, temperature gradient close to the burning surface has a very high value. It implies that thermocouple measurements can give temperature profiles with significant errors due to thermocouple heat inertia. Because of that it is necessary to find conditions under which thermocouple measurements in combustion waves will introduce small errors. These conditions have been found by numerical simulations. The thermocouple partially absorbs the heat of the thermal layer and decreases the temperature at the point of the measurement. The requirement of

small temperature error (less than 10%) of the thermocouple is indicated by the following formula :

$$h<0.2\ \chi/r_b;$$

Here: h - thermocouple thickness (in cm), χ- heat diffusivity of the solid (in cm^2/s), r_b - linear burning rate (in cm/s). $\chi/r_b=l_t$ where l_t is the thickness of the thermal layer of the condensed phase. There is another requirement for correct measurements by thermocouples in combustion waves: the thermocouples have to have U-shape form. It is necessary because of a very high difference between heat conductivity coefficients of metallic thermocouple wire and that of solid or gas. The junctions of U-shaped thermocouples do not experience large temperature decrease. Modelling experiments and numerical simulations show that the decrease of junction temperature will be small (≤3%) if the horizontal part of the U-shaped thermocouple is about one hundred times more than thermocouple thickness h. Thermal inertia of the thermocouple in the gas phase can be taken into consideration and eliminated by a correction procedure. The procedure implies the use of the following equation:

$$dT_{ex}/dx=(r_b\tau_o)^{-1}\cdot(T - T_{ex});$$

Here: T - the real temperature of gas in the combustion wave; T_{ex} - the temperature registrated by thermocouple; τ_o - time response of the thermocouple in gas. Time response depends on mass burning rate m ($m=\rho\cdot r_b$) and on T. The temperature profiles in gas were corrected by this equation. The theory of thermocouple measurements in combustion waves of solids was created and confirmed by measurements of combustion wave temperature profiles by thermocouples with sequentially decreased thickness (method of "zero diameter"). All the above mentioned requirements have been met in the investigations. Different types of metal wires for thermocouples were used (We,Re and Pt,Rh) to test the catalytic effect on thermocouples. The catalytic effect was not observed. The method of burning surface temperature measurement by determining locations of slope breaks on temperature profiles registered by thermocouples (method of "slope break") is based on the existence of the delay ($r_b\tau_o$) on the temperature profiles when thermocouples go through the burning surface. The delay is due to the change of heat exchange between environment and thermocouple: contact heat exchange in solid is replaced by convective heat exchange in gas.

Results and Discussion

A number of mixtures were prepared on the base of HMX and RDX. Powders of HMX and RDX were separated preliminary into groups having restricted particle sizes (50 mkm and less; 50-800mkm; <50mkm/50-800mkm, 50%/50%; and so forth). Then mixtures with these powders were prepared. After polymerization, cylindrical samples of various diameters (5-15mm) were made. The influence on the burning wave parameters of the values of nitramine particle sizes, sample density, degree of polymerisation and amount of oxidizer in the mixtures were preliminary studied. It was shown that mixture density, degree of polymerisation and nitramine particle sizes do not effect significantly mass burning rates and burning wave parameters. However the amount of nitramine content in the mixtures effects significantly all the characteristics. Because of that a detailed investigation was performed for the following mixtures:

No.1. RDX:HTPB1, 80:20 (%, by weight), mixture density $\rho=1{,}35 g/cm^3$; nitramine particle sizes (nps) <100mkm; chemical brutto-formula: $O_{21.76}H_{43.72}N_{21.72}C_{25.27}$;

No.2. RDX:HTPB1, 87:13 (%, by weight), $\rho=1{,}42 g/cm^3$; (nps) <100mkm; chemical brutto-formula: $O_{23.6}H_{37.87}N_{23.57}C_{21.16}$;

No.3. HMX:HTPB1, 80:20 (%, by weight), density $\rho=1{,}5 g/cm^3$; (nps): <30mkm/315mkm (50%/50%); chemical brutto-formula: $O_{21.76}H_{43.72}N_{21.72}C_{25.27}$;

No.4. HMX:HTPB1, 87:13 (%, by weight), density $\rho=1{,}59 g/cm^3$; (nps): <30mkm/315mkm (50%/50%); chemical brutto-formula: $O_{23.6}H_{37.87}N_{23.57}C_{21.16}$;

Cylindrical samples of diameters 5-15mm were protected by thin layer of polymer glue. Temperature profiles and surface temperatures were obtained for indicated mixtures at pressures

1(5), 10, 20 50 and 80atm and at sample temperatures T_o=+20 and +100C°. Stable combustion waves at T_o between -150 and -100C° were not observed.

Carbon Residue After Combustion.

A porous black carbon residue on the burning surface of the mixtures 20:80 (No.1. and No.3.) was observed. The residue of the mixtures holds the shape of sample after combustion at 1-20atm. The measured density of carbon residue for the mixtures 20:80 comprises about 0.1g/cm^3 at 1atm, about 0.01g/cm^3 at 20atm and less than 0.01g/cm^3 at 50atm.

The mixtures 13:87 (No.2. and No.4.) practically have no carbon residue.

Figs.1-10 show averaged temperature profiles (averaging from 6-12 temperature curves for every regime of combustion). Tables 1-4 show the averaged burning wave parameters obtained by experiments and by processing experimental data (see below). Standard deviation of mass burning rate (m) measurement is ϑm=±5%. Standard deviation of burning surface temperature (T_s) measurement is ϑT_s=±5%.

Mass burning rate.

It can be seen that mass burning rate m increases when pressure increases, when sample temperature T_o increases and, as a rule, when amount of oxidizer increases (exclusion for RDX-mixtures, T_O=+100°C, is connected, presumably, with especially low mixture density and, may be, with not very good sample side protection from the flame penetration for the mixture 80:20 at T_o=+100°C). Mass burning rate of RDX-mixtures are always higher than that of HMX-mixtures. Values of m for the studied mixtures comprise values from 0.05 to 0.4-1.2g/cm^{2}s.

Burning Surface Temperature.

It can be seen that burning surface temperature T_s always increases when m increases. Because of that the same conclusions can be made for T_s: burning surface temperature increases when pressure increases, when sample temperature T_o increases and, as a rule, when amount of oxidizer increases. Values of T_s comprise values from 305 to 485°C.

Temperature Profiles.

Figs.1-20 show that at pressures 10-20(50)atm the gas phase of the combustion waves has two-zone structure: the first zone with mean zone temperatures T_1 and the second zone (flame zone) with the final zone temperatures T_f. Both zones merge at 50(80)atm. At 1atm exists only the first zone with the final zone temperature T_1. Standard deviation of the first zone temperature (T_1) measurement is ϑT_1=±10% and that of the flame zone is ϑT_f=±5%. Values of T_1 comprise values from 800°C to 1150°C for mixtures 20:80, and from 900°C to 1550-1660°C - for mixtures 13:87. Thermodynamically calculated values of T_f are achieved at 50-80atm. Distances L_1 between the burning surface and the beginning of the flame zone (in fact, L_1 is the length of the first flame) change from 3.5-4mm at 1atm to 0.5-1mm at 50atm for mixtures 20:80, and from 1.3-3mm at 5atm to 0.35-0.8mm at 50atm - for mixtures 13:87. Distances L between the burning surface and the flame (up to 0.95T_f; in fact, L is the length of the gas phase reaction zone) change from 2.5-3mm at 10atm to 1-1.6mm at 80atm for mixtures 20:80, and - from 2.5-3mm at 5atm to 0.6-1mm at 80atm - for mixtures 13:87. Standard deviations of L_1 and L are ±15%.

Characteristic Sizes in Gas and Solid, and Heat Diffusivity of Heat Layer in Solid.

Characteristic thickness l_t and l_m in solid in Tables 1-4 was obtained by temperature distributions in solid. Experimentally obtained thickness of heat layer in solid l_t is the distance between the burning surface and the section in solid with temperature $T^*=(T_s-T_o)/e - T_o$ (e is the base of natural logarithm). It was assumed here that the section of heat release in solid resides close to the surface in the thin layer and practically all the thickness of the region of the changed temperature in solid is the heat layer. The assumption was based on the results of the measurements of temperature profile in solid which show that the heat diffusivity obtained by formula $\chi=l_t \cdot r_b$ is equal to the value obtained for the solid by other methods. The values l_t obtained by temperature profiles (see Tables 1-4) allow the mean values of the heat diffusivity of heat layer in solid to be estimated. As a rule at 1-5atm (T_s≈300-350°C) for all mixtures $\chi=1\cdot10^{-3}$cm^2/s, at 10-20atm (T_s≈360-400°C) - $\chi=(1.5\text{-}2)\cdot10^{-3}$cm^2/s and at 20-80atm ($T_s$≈410-480°C) - $\chi=(2\text{-}3)\cdot10^{-3}$cm^2/s. Thickness of the melted layer in solid l_m was obtained by nitramine melting

temperatures T_m which are equal to 200°C for RDX and 280°C for HMX. Tables 1-4 show that l_m decreases for RDX-mixture (20:80) from 150-170mkm at 1atm to 50-60mkm at 80atm, for HMX-mixture (20:80) from 50mkm at 1atm to 35-40mkm at 80atm, for RDX-mixture (13:87) from 95-100mkm at 5atm to 33-45mkm at 80atm, for HMX-mixture (13:87) from 45-42mkm at 5atm to 22-25mkm at 80atm. The temperature profile in solid at 1atm has thick melted layer l_m=170mkm which can be seen even by the shape of this profile (see Fig.1 and Fig.6).

We determine characteristic size of the gas phase l_g on the temperature profiles as the thickness at which the temperature gradient φ decreases e-times beginning from the burning surface. Tables 1-4 show the obtained values l_g. It can be seen that at 1atm l_g are equal to 1.4-1.8mm and at the elevated pressures l_g comprise values from 260-420mkm at 10atm up to 100-200mkm at 80atm for mixtures 20:80, and values from 250-350mkm at 5atm up to 120-160mkm at 80atm - for mixtures 13:87. These are very large values.

For detailed analysis of the physics of combustion of these mixtures it is important to estimate the conductive size ψ of the gas phase of the investigated combustion waves. The conductive size ψ can be obtained by the following formula: $\psi=\lambda_1/mc_p$; where λ_1 is the heat conductivity of the gas phase and c_p is the specific heat of the gas phase. Tables 1-4 show the obtained values ψ. It can be seen that values ψ decrease from 63-72mkm at 1atm to 4.2-7.1mkm at 80atm for RDX-mixture 20:80, from 74-91mkm at 1atm to 6.8-11.3mkm at 80atm - for HMX-mixture 20:80, from 32-48mkm at 5atm to 4.9-5.1mkm at 80atm - for RDX-mixture 13:87, and from 22.7-25.5mkm at 5atm to 4.4-4.9mkm at 80atm - for HMX-mixture 13:87. It is obvious that $\psi<<l_g$.

Heat Release in Solid and Heat Feedback from Gas to Solid.

The obtained temperature profiles and burning surface temperature allow the thermal burning wave structure to be estimated. First of all we can obtain values of heat release in solid and heat feedback from gas to solid. Heat flux from gas to solid $q\cdot m$ by heat conductivity is as follows:

$$q\cdot m=-\lambda_1(T)\cdot(dT/dx)_o;$$

Here: λ_1 is coefficient of heat conductivity of the gas phase, $(dT/dx)_o=\varphi$ is the temperature gradient in gas close to the burning surface. Heat feedback from gas into solid by heat conductivity q is as follows:

$$q=-\lambda_1(T)\cdot\varphi/m;$$

Heat release in the reaction layer of the condensed phase (or on the burning surface) Q is as follows:

$$Q=c\cdot(T_s-T_o)-q+q_m;$$

Where c is coefficient of solid specific heat and q_m is the heat of nitramine melting: q_m=28x0.8cal/g for mixtures 20:80 and q_m=28x0.87cal/g for mixtures 13:87. The standard deviations of Q and q are equal to ±10% and 20%, correspondingly. Table 5 shows the used functions $\lambda_1(T)$, c(T) and $c_p(T)$. Tables 1-4 show that the temperature gradient φ in gas close to the burning surface has very large values especially in mixtures 13:87: it can be as much as 10^5K/cm. The general conclusion about the heat release in solid and the heat feedback from gas to solid in combustion waves of the studied polymer-nitramine mixtures is as follows: strong heat release in solid and weak heat feedback from gas to solid are observed for all of the studied regimes. Indeed Q is equal to 81-159cal/g and q is equal to 5.3-21.5cal/g. It is important to stress that Q increases when pressure and m increase. And q can decrease when pressure and m increase (at p>20-50atm). Values Q and q increase when amount of oxidizer (nitramine) in mixture content increases. Q decreases when T_o increases. The mixtures on the base of RDX have the higher values Q than that of the mixtures on the base of HMX.

Heat Release Rate in Gas Close to Burning Surface.

The temperature profiles and burning surface temperature allow heat release rates Φ_o in gas close to the surface to be estimated. Φ_o shows, obviously, the intensity of chemical reactions in gas. Values Φ_o were obtained from the heat conductivity equation and the temperature profiles. The heat conductivity equation connected with the burning surface for the gas phase of stable propagated combustion wave is as follows:

$$d/dx\cdot(\lambda_1 dT/dx)-m\cdot c_p\cdot dT/dx+\Phi(x)=0;$$

Here $\Phi(x)$ is the distribution of the heat release rate in the gas phase of the combustion wave. The first term of the equation at $x \approx 0$ is small and thus the following expression for $\Phi(x \approx 0)=\Phi_o$ is valid:

$$\Phi_o = c_p \cdot m \cdot \varphi;$$

The standard deviation of Φ_o is equal, as a rule, to 20-30%. Tables 1-4 show that the values Φ_o are very high and can comprise 33,8·*K*cal/cm^{3}s. Φ_o increases when pressure, amount of nitramine and T_o increase. The mixtures with RDX have, as a rule, higher values Φ_o than those of the mixtures with HMX.

Table 1

Burning Wave Parameters of Mixture RDX:HTPB1, 80:20

	p, atm	1		10		20		50		80	
	T_o,°C	20	+100	20	+100	20	+100	20	+100	20	+100
1	m,g/cm^{2}s	0.05	0.06	0.18	0.42	0.27	0.62	0.48	0.97	0.65	1.16
2	T_s,°C	305	310	350	410	370	440	430	475	445	486
3	$\varphi \cdot 10^{-4}$,K/cm	0.4	0.3	2.4	1.9	4.0	3.0	6.8	3.6	4.0	4.5
4	q, cal/g	8.0	5.3	15.0	5.3	17.5	6.5	18.8	5.3	8.4	5.7
5	Q, cal/g	101	81	109	113	113	123	132	136	148	139
6	l_t, mkm	260	220	120	70	90	55	70	40	70	40
7	l_m, mkm	170	150	80	80	75	75	50	60	60	50
8	L_1, mm	4.0	4.0	1.3	1.8	0.75	1.0	-	0.6	-	-
9	T_1,°C	800	820	900	950	950	1000	-	1100	-	-
10	L, mm	-	-	2.5	3.0	2.0	2.5	1.2	2.0	1.0	1.5
11	T_f,°C	-	-	1480	1500	1500	1600	1500	1600	1500	1600
12	l_g, mkm	1400	1800	260	260	230	250	220	140	200	120
13	ψ, mkm	72	63	22.6	10.7	15.6	7.4	9.3	5.0	7.1	4.2
14	Ω	20	28	12	24	15	34	24	28	28	29
15	Φ_o,*K*cal/cm^{3}s	0.055	0.05	1.2	2.3	3.1	5.4	9.5	10.3	7.6	15.6

Table 2

Burning Wave Parameters of Mixture HMX:HTPB1, 80:20

	p, atm	1		10		20		50		80	
	T_o,°C	20	+100	20	+100	20	+100	20	+100	20	+100
1	m,g/cm^{2}s	0.04	0.05	0.10	0.15	0.16	0.24	0.29	0.53	0.38	0.70
2	T_s,°C	300	305	325	340	340	370	380	440	400	455
3	$\varphi \cdot 10^{-4}$,K/cm	0.55	0.55	1.7	1.8	2.6	2.8	4.5	3.5	6.0	4.4
4	q, cal/g	13.8	11.0	18.4	13.2	18.0	13.5	18.6	8.9	19.8	7.8
5	Q, cal/g	94	77	98	83	103	93	115	120	121	127
6	l_t, mkm	270	200	160	160	140	120	95	60	90	50
7	l_m, mkm	50	50	40	60	40	50	30	35	40	35
8	L_1, mm	3.5	3.5	1.2	1.5	0.80	1.0	0.5	1.0	-	-
9	T_1,°C	800	850	880	950	950	1050	1050	1150	-	-
10	L, mm	-	-	2.5	3.0	1.8	2.5	1.3	2.0	1.2	1.6
11	T_f,°C	-	-	1470	1540	1480	1580	1490	1590	1500	1600
12	l_g, mkm	1400	1600	400	420	320	250	160	200	100	120
13	ψ, mkm	91	74	37.8	26.2	24.0	17.5	14.5	8.7	11.3	6.8
14	Ω	15	22	11	16	13	14	11	23	9	18
15	Φ_o,*K*cal/cm^{3}s	0.06	0.076	0.47	0.76	1.16	1.92	3.75	5.5	6.6	9.1

Table 3

Burning Wave Parameters of Mixture RDX:HTPB1, 87:13

	p, atm	5		10		20		50		80	
	T_o,°C	20	+100	20	+100	20	+100	20	+100	20	+100
1	m,g/cm²s	0.10	0.14	0.15	0.23	0.27	0.42	0.63	0.74	0.95	0.99
2	T_s,°C	325	350	350	365	375	410	445	460	475	477
3	$\varphi \cdot 10^{-4}$,K/cm	1.9	3.0	2.8	3.6	5.0	5.2	8.0	8.5	10.5	11.5
4	q, cal/g	20.5	24.6	21.5	18.5	22.0	16.0	16.5	16.0	16.6	16.8
5	Q, cal/g	98	77	105	88	112	105	142	122	152	127
6	l_t, mkm	145	100	140	93	80	65	50	42	37	36
7	l_m, mkm	100	95	92	90	60	75	40	50	33	45
8	L_1, mm	1.8	2.0	1.3	1.6	0.8	1.2	0.6	0.8	-	-
9	T_1,°C	900	960	1000	1040	1100	1150	1600	1660	-	-
10	L, mm	2.8	3.0	2.0	2.6	1.7	2.0	1.0	1.1	0.6	0.7
11	T_f,°C	1350	1450	1600	1650	1800	1850	1900	1950	1900	1950
12	l_g, mkm	300	250	220	200	180	170	180	140	130	120
13	ψ, mkm	40.8	32	29.3	18.3	15.5	10.6	7.0	6.4	5.1	4.9
14	Ω	7.3	8.0	7.5	11	12	16	26	22	25	24
15	Φ_o,*K*cal/cm³s	0.5	1.2	1.2	2.4	3.8	6.3	14.8	18.6	29.6	33.8

Table 4

Burning Wave Parameters of Mixture HMX:HTPB1, 87:13

	p, atm	5		10		20		50		80	
	T_o,°C	20	+100	20	+100	20	+100	20	+100	20	+100
1	m,g/cm²s	0.16	0.18	0.20	0.24	0.27	0.32	0.48	0.56	1.00	1.10
2	T_s,°C	350	355	360	370	375	390	420	435	480	485
3	$\varphi \cdot 10^{-4}$,K/cm	3.0	2.0	3.6	3.5	4.4	5.0	6.4	7.6	8.0	9.2
4	q, cal/g	21.5	12.8	21.0	17.5	19.6	19.5	17.3	18.3	11.6	12.0
5	Q, cal/g	104	90	108	91	115	95	133	112	159	135
6	l_t, mkm	150	100	120	95	90	86	66	58	45	40
7	l_m, mkm	45	42	42	40	38	36	30	28	25	22
8	L_1, mm	1.3	2.0	1.0	1.4	0.6	1.0	0.35	0.8	-	-
9	T_1,°C	880	920	970	1050	1080	1180	1450	1550	-	-
10	L, mm	2.5	3.0	2.5	2.6	1.6	2.0	1.2	1.2	1.0	0.9
11	T_f,°C	1300	1350	1500	1600	1700	1780	1860	1900	1870	1900
12	l_g, mkm	250	350	220	240	200	200	150	130	160	120
13	ψ, mkm	25.5	22.7	20.0	17.7	15.5	13.0	9.3	8.0	4.9	4.4
14	Ω	10	15	11	14	13	17	16	16	33	27
15	Φ_o,*K*cal/cm³s	1.35	1.0	2.0	2.4	3.4	4.6	9.0	12.5	23.8	30.1

Table 5

Thermophysical coefficients, nitramine-polymer mixtures

T,°C	300	350	400	450	500	550	600
c, cal/g·K	0.305	0.308	0.312	0.316	0.320	0.322	0.325
$\lambda_1 \cdot 10^4$,cal/cm·s·K	1.00	1.15	1.25	1.38	1.50	1.62	1.75
c_p cal/g·K	0.275	0.282	0.290	0.295	0.300	0.305	0.310

Burning Rate Control Region in the Combustion Waves.

The results of measurements q and Q show that the main factor of the creation of the burning rate of the studied mixtures is heat release in solid (or on solid surface) and, in a smaller degree, heat feedback from the gas layer adjacent to the surface. The following conclusion can be made from the analyses of the obtained data: the high temperature region of the burning waves cannot affect the burning rate. Indeed the influence of the heat release in the gas phase of the burning wave on the burning rate can be estimated by the following formula obtained as a solution of the heat conductivity equation:

$$m \cdot q = \int_0^\infty \Phi(x) \cdot \exp(-x/\psi) \cdot dx;$$

Here $\Phi(x)$ is the distribution of the heat release rate in the gas phase of the burning wave (see above). This equation shows that the influence of the heat release in gas on the burning rate decreases very quickly when x exceeds ψ. It implies that the heat release in gas does not affect the burning rate beginning from $x>\psi$. Tables 1-4 show that the values ψ are very small and they are much smaller than the characteristic size of the gas phase l_g - see values Ω in the Tables ($\Omega=l_g/\psi$). It can be seen that Ω is equal to 7-33. It implies that only a very thin layer in the gas phase close to the burning surface can be responsible for the burning rate.

Thus the obtained results show that the burning rate control region in the studied combustion waves for all the regimes of combustion is the region of heat release in solid just under the burning surface (or immediately on the burning surface) and a very thin low-temperature gas layer close to the burning surface which has the thickness $\sim\psi$. High temperature gas regions cannot influence the burning rate because of a very large heat resistance of the main volume of the gas phase.

Macrokinetics of Solid Gasification in Combustion Waves.

The following equation connects burning rate of solid with burning surface temperature and with macrokinetic characteristics of solid gasification:

$$m^2=\lambda\rho/Q^2 \cdot \Re T_s^2/E \cdot 1/N \cdot \exp(-E/\Re T_s);$$

Here $N=1/\eta_s + (1-\eta_s)/\eta_s \cdot \ln(1-\eta_s) - (q/Q) \cdot [\ln(1-\eta_s)]/\eta_s$; $\eta_s=Q/Q^*$; Q^* is the maximum heat release in solid (for polymer-nitramine mixture combustion waves $N\cong1$); λ is solid heat conductivity, E is activation energy of limiting stage of the gasification process.

This expression was obtained by the solution of the system of two equations for the steady propagated burning wave: the heat conductivity equation for solid phase and the equation of diffusion of reagents. The burning wave propagates due to heat release in solid Q and heat feedback from gas to solid q. Function of the volumetric heat release rate Φ_c in solid was assumed as follows:

$$\Phi_c(\eta, T)=Q^* k_o \cdot \rho \cdot (1-\eta) \cdot \exp(-E/\Re T);$$

Here η is the reaction completeness ($\eta=\eta_s$ on the burning surface), k_o is the preexponent multiplier.

Calculations show that the simplified macrokinetic laws of gasification in the combustion waves of the studied mixtures have the following forms:

No.1. RDX:HTPB1, 80:20; $m=5.78 \cdot 10^3 \cdot \exp(-25{,}800/2\Re T_s)$, g/cm^{2}s;

No.2. RDX:HTPB1, 87:13; $m=7.24 \cdot 10^3 \cdot \exp(-26{,}600/2\Re T_s)$, g/cm^{2}s;

No.3. HMX:HTPB1, 80:20; $m=4.47 \cdot 10^3 \cdot \exp(-25{,}500/2\Re T_s)$, g/cm^{2}s;

No.4. HMX:HTPB1, 87:13; $m=6.26 \cdot 10^3 \cdot \exp(-26{,}300/2\Re T_s)$, g/cm^{2}s;

Here T_s in K, m in g/cm^{2}s; $\Re$ is the gas constant.

One of the merits of these laws are the possibility of estimations of values T_s under different conditions by using experimentally obtained values of mass burning rates m.

It is necessary to stress that all the obtained macrokinetic laws of solid gasification in combustion waves for the studied mixtures are similar.

Temperature Sensitivities of Mass Burning Rate and Surface Temperature.

Temperature sensitivities of burning rate and surface temperature are important characteristics of solid combustion. The following temperature sensitivities were found:

$\beta=(\partial \ln m/\partial T_o)_{p\text{-const}}$ - temperature sensitivity of mass burning rate;

$r=(\partial T_s/\partial T_o)_{p\text{-const}}$ - temperature sensitivity of burning surface temperature;

Table 6 shows the obtained values β and r. The temperature interval was 20°C - +100°C.

Table 6

Values of Temperature Sensitivities

mixtures	p, atm	5	10	20	50	80
RDX:HTPB1	β, %/K	37.5(1atm)	45.6	44.3	35.6	30.0
80:20	r	0.06(1atm)	0.75	0.88	0.56	0.52
RDX:HTPB1	β, %/K	18.0	22.5	23.8	8.8	3.1
87:13	r	0.3	0.19	0.44	0.3	0.03
HMX:HTPB1	β, %/K	13.0(1atm)	21.0	22.0	32.0	33.8
80:20	r	0.06(1atm)	0.19	0.38	0.75	0.69
HMX:HTPB1	β, %/K	6.3	10	9.4	8.1	5.0
87:13	r	0.06	0.13	0.19	0.19	0.06

Table 6 shows that only mixtures 87:13 have a normal dependence $\beta(p)$. The characteristic feature of the normal dependence $\beta(p)$: β increases when p increases at low pressures and β significantly decreases at elevated pressures. As a rule, β achieves maximum at 10-20atm and then constantly decreases. Namely this type of dependence is observed for mixtures nitramine-polymer 87:13. However HMX-mixtures 80:20 has constantly increasing dependence $\beta(p)$ and RDX-mixture 80:20 has too large values β. Values r are also larger for mixtures 80:20.

The main conclusion here is as follows: the increase of the amount of oxidizer in these mixtures decreases r and β for both oxidizers.

Conclusions and Recommendations

The study of the combustion mechanism of the mixtures RDX:HTPB1 and HMX:HTPB1 with different values of oxidizer was performed by microthermocouple methods. Temperature profiles and burning wave parameters were obtained under changes of external parameters - initial sample temperature and pressure. Characteristic features of the combustion mechanism of the studied mixtures were established. During the study the following parameters were obtained: burning rates, burning surface temperatures, heat release in solid, heat feedback from gas to solid, first zone and flame zone temperatures and thickness, thickness of heat layer and melted layer in solid, characteristic thickness of the gas phase, macrokinetic parameters of the solid gasification, temperature sensitivities of the burning rate and the burning surface temperature. It was established that the significant heat release in solid and the weak heat feedback from gas to solid take place. The control region in the combustion waves which governs the burning rate is placed in solid and in a thin gas layer close to the surface. Macrokinetic laws of solid gasification for all mixtures are similar. The increase of the amount of nitramines in the mixtures decreases temperature sensitivities of burning rate and burning surface temperature.

The recommendation: it is necessary to obtain and to analyse the pointed above characteristics for mixtures: nitramines - energetic binders, like GAP, BAMO etc.

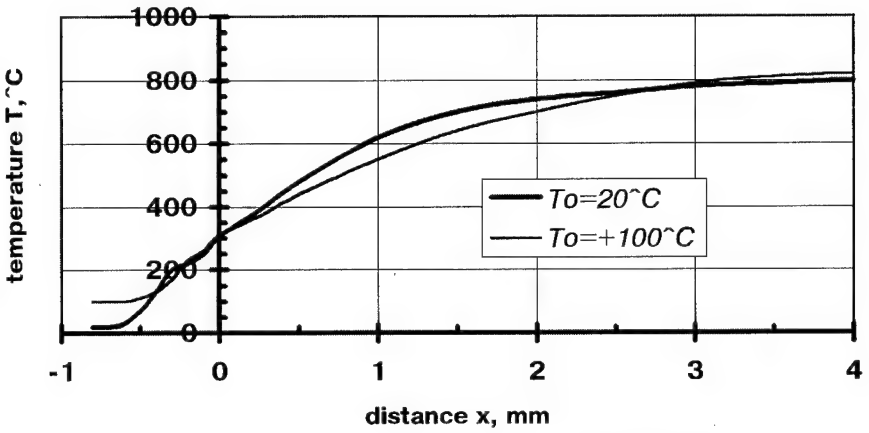

Fig.1. Temperature profiles T(x). RDX-HTPB1, 80:20. 1atm.

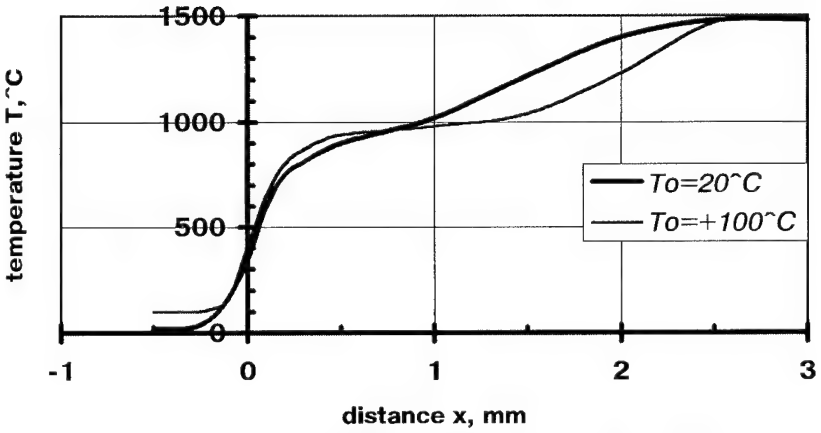

Fig.2. Temperature profiles T(x). RDX-HTPB1, 80:20. 10atm.

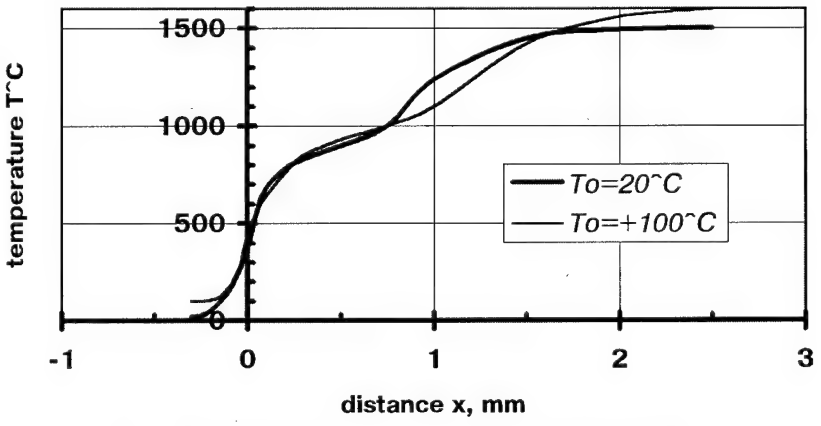

Fig.3. Temperature profiles T(x). RDX-HTPB1, 80:20. 20atm.

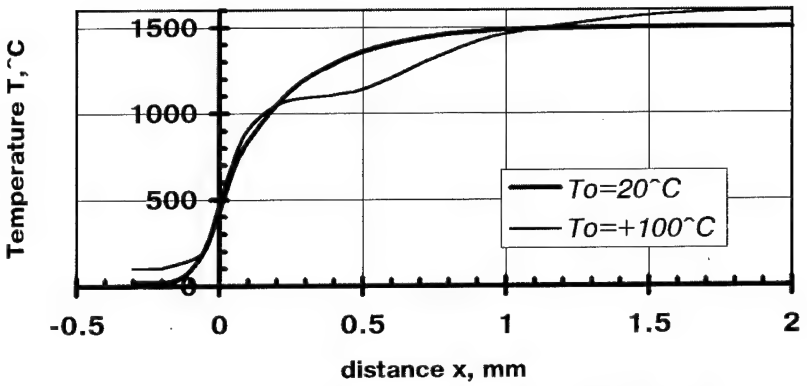

Fig.4. Temperatere profiles T(x). RDX-HTPB1, 80:20. 50atm.

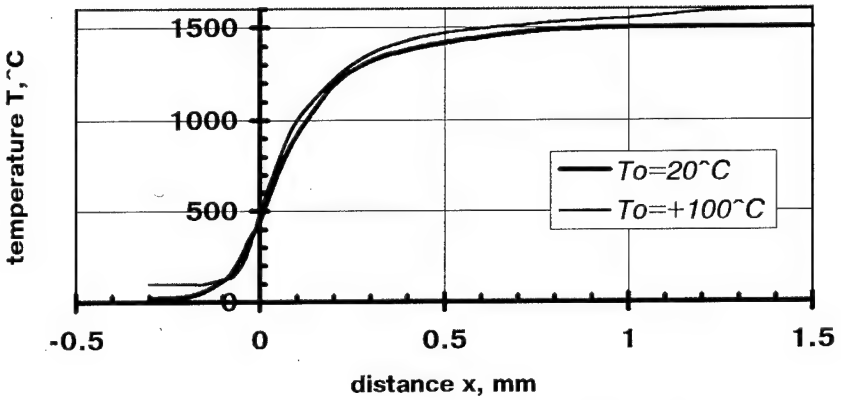

Fig.5. Temperature profiles T(x). RDX-HTPB1, 80:20. 80atm

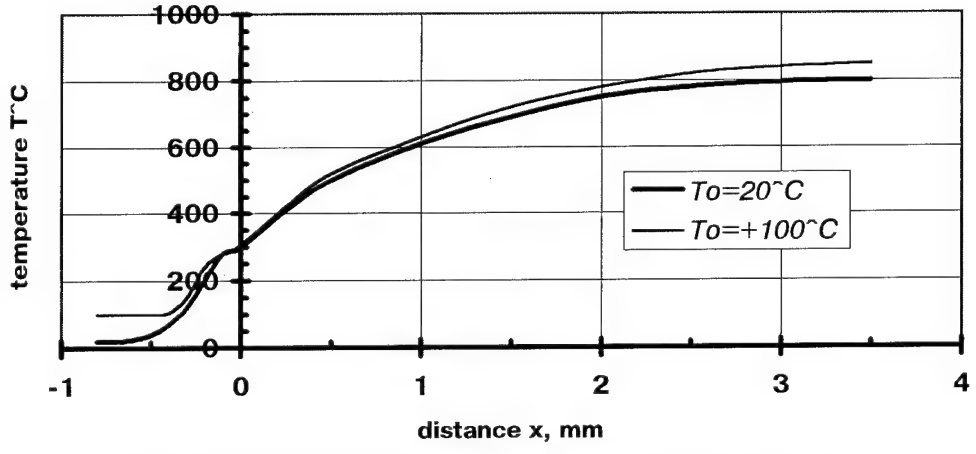

Fig.6. Temperature profiles T(x). HMX-HTPB1, 80:20. 1atm.

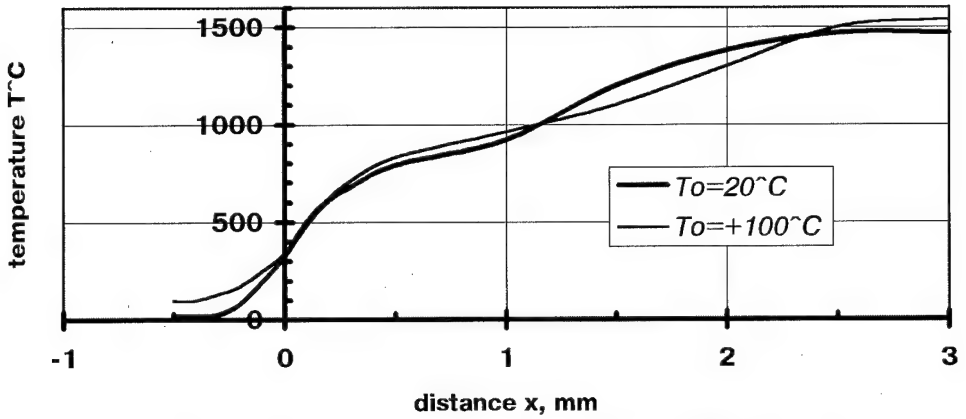

Fig.7. Temperature profiles T(x). HMX-HTPB1, 80:20. 10atm.

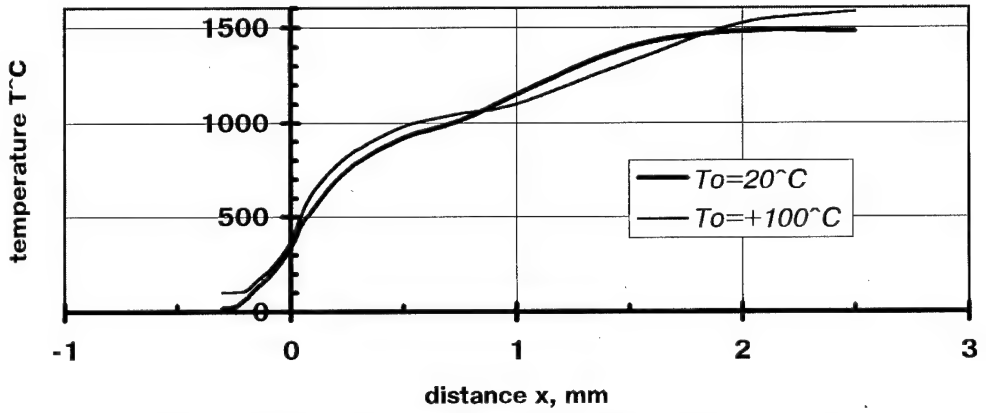

Fig.8. Temperature profiles T(x). HMX-HTPB1, 80:20. 20atm.

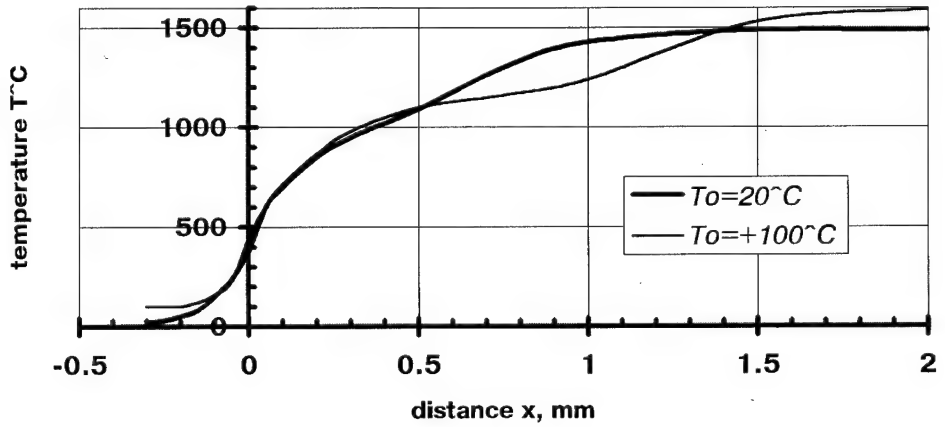

Fig.9. Temperature profiles T(x). HMX-HTPB1, 80:20. 50atm.

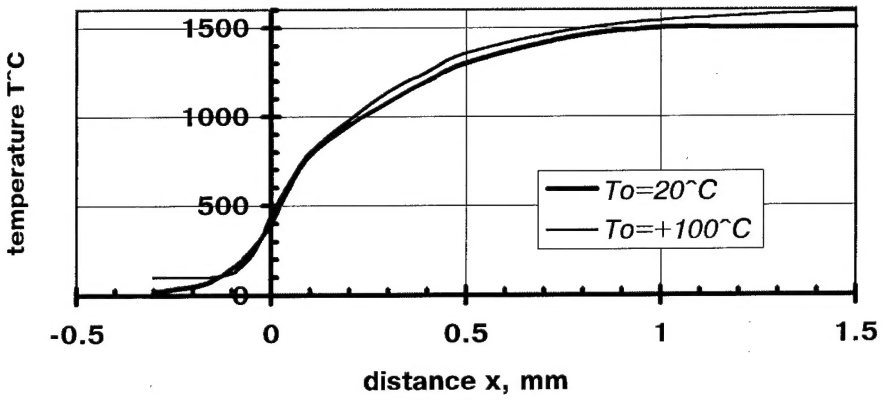

Fig.10. Temperature profiles T(x). HMX-HTPB1, 80:20. 80atm.

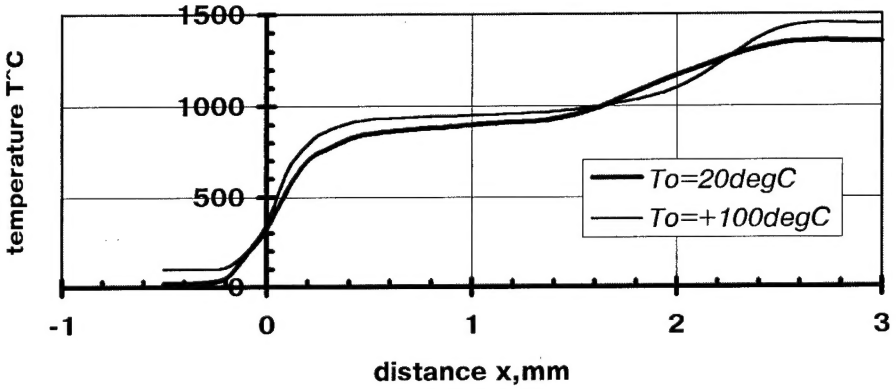

Fig.11. Temperature Profiles T(x). RDX-HTPB1, 87:13. 5atm

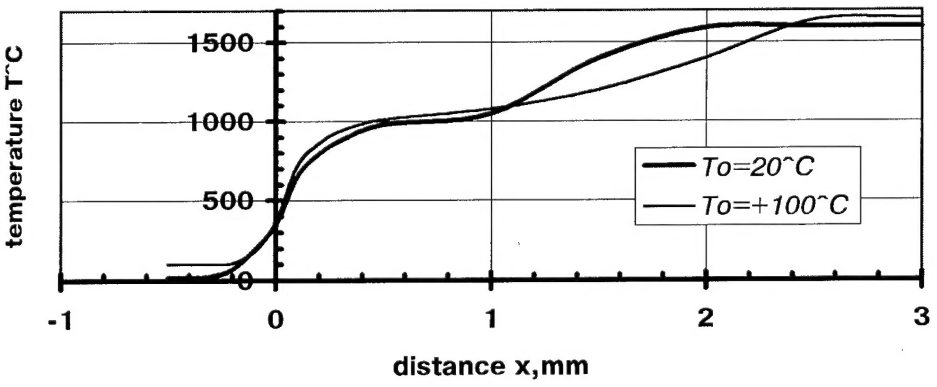

Fig.12. Temperature Profiles T(x). RDX-HTPB1, 87:13. 10atm

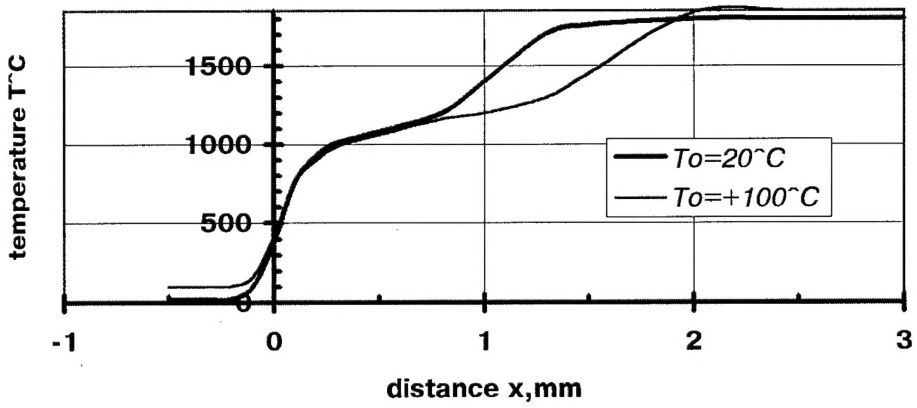

Fig.13. Temperature Profiles T(x). RDX-HTPB1, 87:13. 20atm

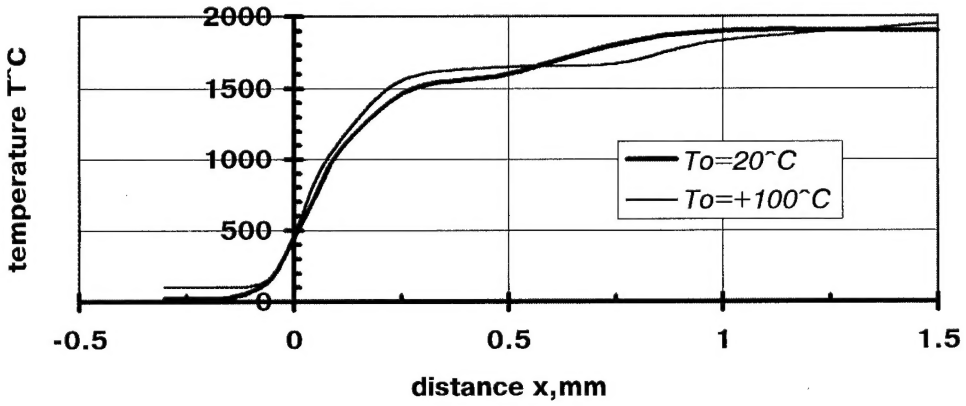

Fig.14. Temperature Profiles T(x). RDX-HTPB1, 87:13. 50atm

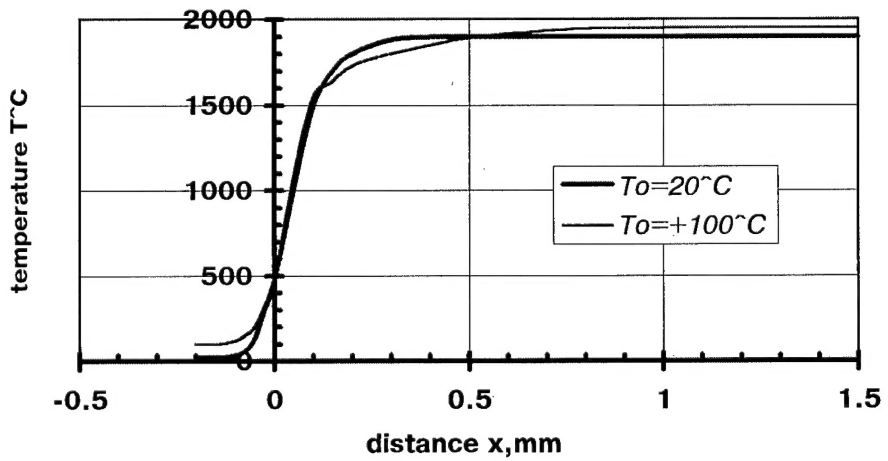

Fig.15. Temperature Profiles T(x). RDX-HTPB1, 87:13. 80atm

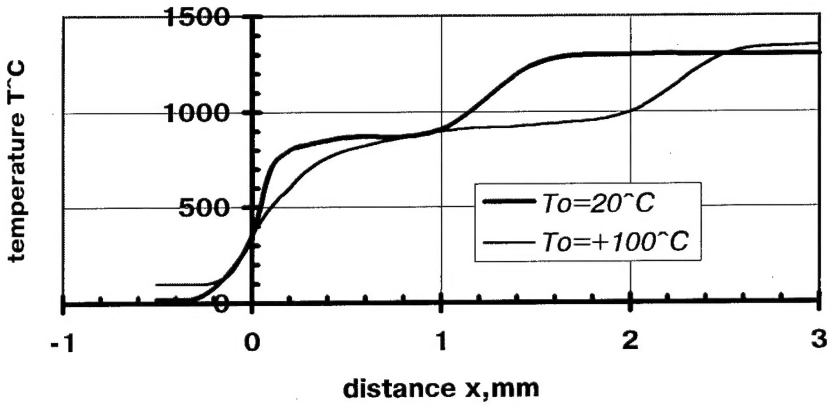

Fig.16. Temperature Profiles T(x). HMX;HTPB1, 87:13. 5atm

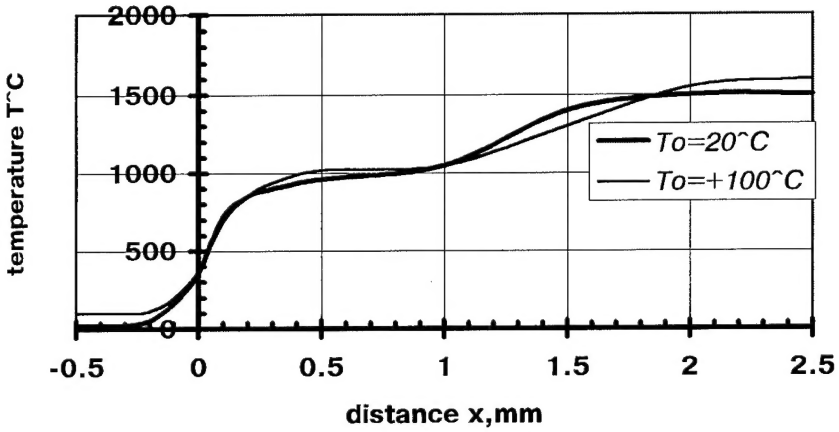

Fig.17. Temperature Profiles T(x). HMX-HTPB1, 87:13. 10atm

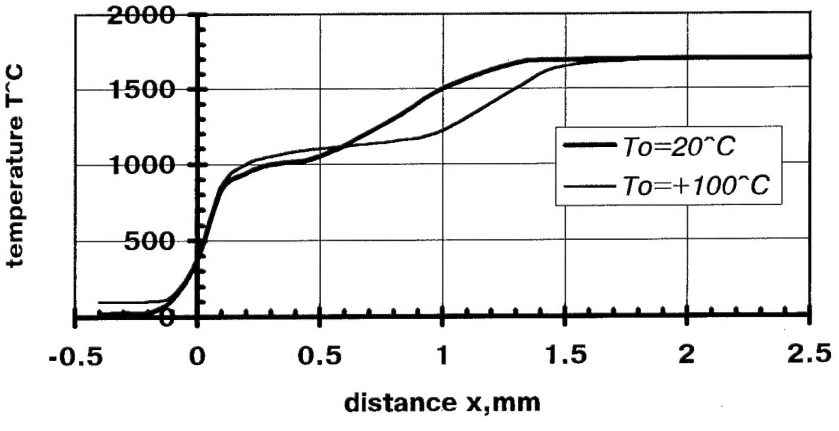

Fig.18. Temperature Profiles. HMX-HTPB1, 87:13. 20atm

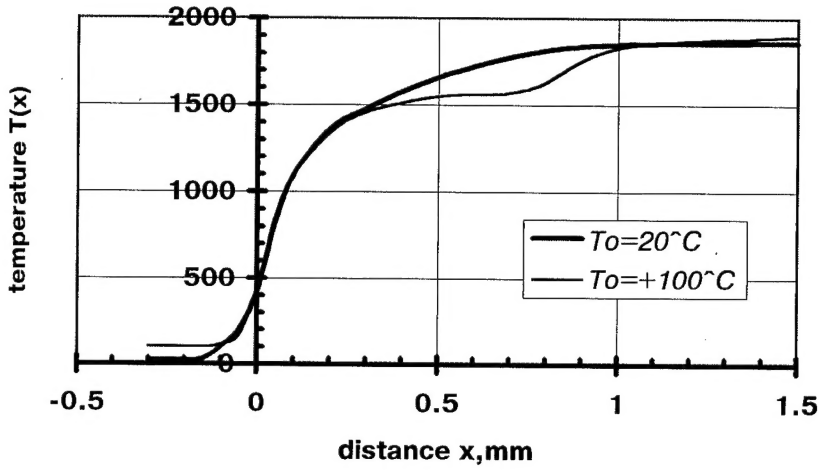

Fig.19. Temperature Profiles. HMX-HTPB1, 87:13. 50atm

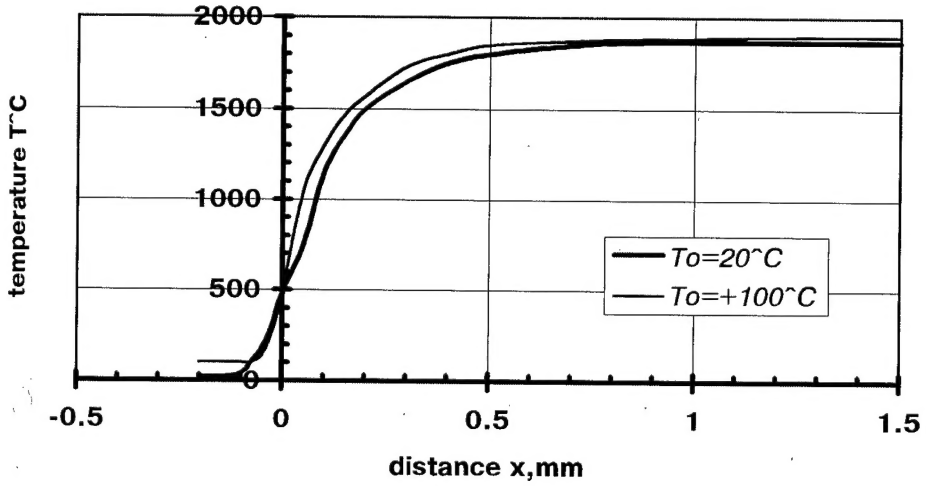

Fig.20. Temperature Profiles. HMX-HTPB1, 87:13. 80atm